Evaluation of metallization-induced losses in PERC solar cells using micro-photoluminescence imaging technique

Supawan Joonwichien, Katsuhiko Shirasawa, Hidetaka Takato
産業技術総合研究所　再生可能エネルギー研究センター　太陽光チーム

Metallization-induced losses in rear-side of PERC [1]

We demonstrate and discuss the metallization-induced recombination losses at the rear side of PERCs evaluated by micro-photoluminescence imaging technique.

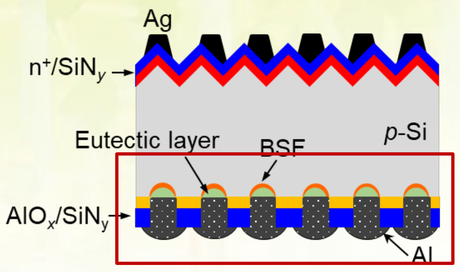

A. Losses associated with Si within passivation layers

The level of surface passivation can be modified by adjusting the compositions of the SiN_y films where compositions of Si, H, and N can be described with respect to the refractive index (n).

Film properties of AlO_x/SiN_y stacks after firing.

B. Losses associated with Si present within the Al paste

The amount of Si in the Al paste has significant effect on solar cell parameters.

Experimental[2]

Bifacial PERCs with different rear Al grid widths were used as test device models.

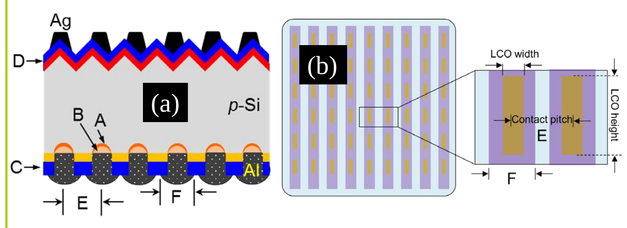

We completed the bifacial metallization by the Al grid screen-printing of commercial Al PERC paste directly on top of the ablated local contact. The printed line widths (F) were 80 µm, 130 µm, and 180 µm, respectively.

Fig. 1 (a) Cross-sectional diagram (not to scale) of the *p*-type Bi-PERC. (b) Sketched rear side of Bi-PERC, showing dash-shaped local contacts and with Al-grid-printed contacts.
A: Al-BSF. B: Local contact site. C: AlO_x/SiN_y passivation stacks. D: SiN_y antireflection coating films. E: Distance between Al grids. F: Width of Al grid.

Results[2]

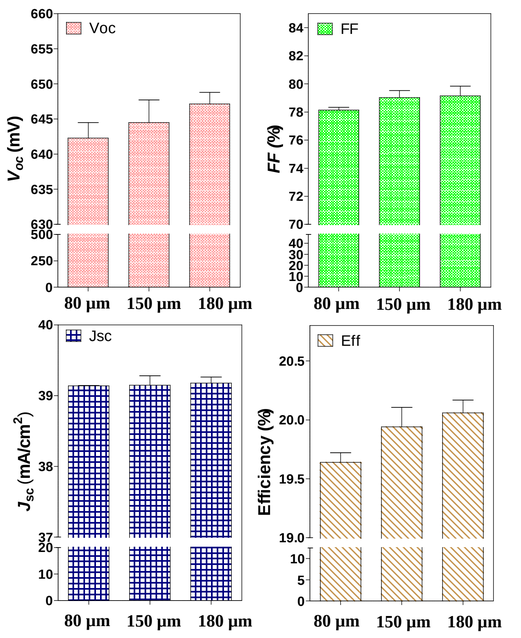

Fig. 2 Correlation between solar cell parameters and the width of Al grid contact (F).

- The results clearly show increases in the V_{oc}, FF, and conversion efficiency values with the widened finger width.
- The change in J_{sc} was negligible, suggesting that fraction of metallization areas on rear side of Bi-PERCs does not significantly affect the internal optical reflection inside the cell.
- The mean FF slightly improved, in which the Al grid for bifacial concept directly influences the series resistance as the finger dimensions and resistivity determines the resistance of the metal electrodes.
- From our earlier work [1], the resulting of thicker Al-BSF induced by a widen Al grid is not the only one reason for the improved V_{oc}.

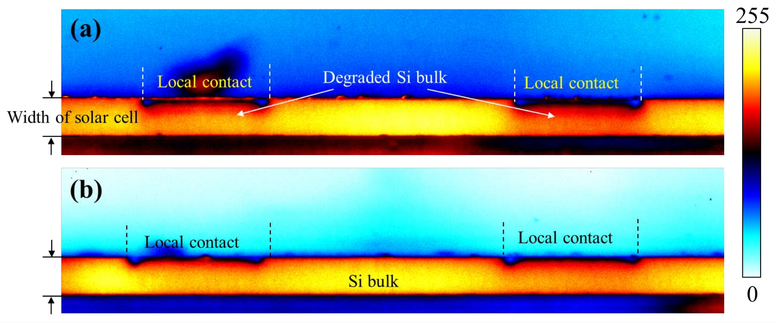

Fig. 3 Comparison of the cross-sectional micro-PL image of Bi-PERC metallized with (a) 80-µm Al-grid width, and (b) 180-µm Al-grid width, respectively, showing the Si substrate and local contact site.

- With focusing on the regions under local contact, PL contrast decreased compared to the PL contrast at the neighbor regions adjacent to the local contact for both samples.
- When the wider Al grid was used (Fig. 3b), higher PL signals below the local contact were observed, indicating the lower carrier recombination activities at Si substrate.
- The results of micro-PL imaging suggest that the dimension of Al grid for bifacial structure had impacted on not only the local contact formation, and surface passivation quality (as realized by other imaging techniques in our earlier works [1], [3]), but also the final quality of Si substrate directly under local contact areas.

Discussion: possible physical mechanism based on imaging technique[2]

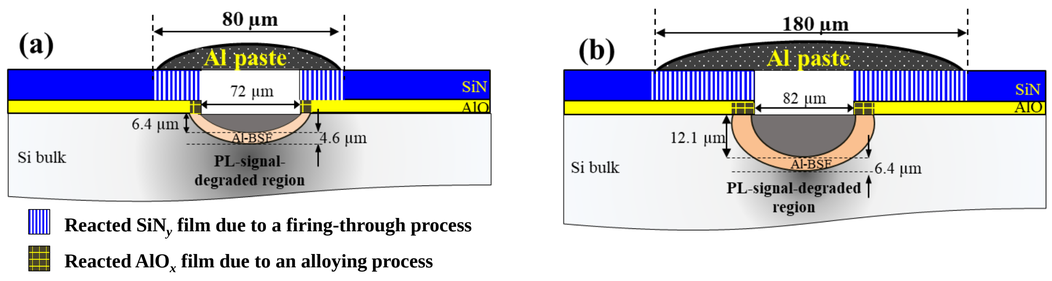

Fig. 4 Schematic drawing of local contact formation in the Bi-PERC metalized with (a) 80-µm Al-grid width, and (b) 180-µm Al-grid width, respectively. Image not to scale.

The micro-PL imaging technique can be used to measure the quantitative carrier recombination lifetime of the finished cells. The structural disorder and electron-hole recombination via band-tail states in amorphous Si and its alloys can be clarified using the PL technique [4]-[10].

- For wider Al grid width 180 µm, the saturation process of the Si in liquid Al within the local contact is slower than the narrower Al grid width. This resulted in the larger contact depth accompanied by a thicker Al-BSF thickness [1], [11].
- The thicker Al-BSF has enabled a strong lateral current from front contacts to local rear contact. However, there were unavoidable events of a local penetration of Al from the paste into the SiN_y film beneath the printed Al grid regions during contact firing. This led to higher fractions of contaminated SiN_y film areas for wider Al grid width, thereby a degraded V_{oc}.
- In Fig. 4, micro-PL image for narrower Al grid width provided new evidence of that the alloying process during metallization also degraded the quality of Si substrate with high recombination centers located at the regions beneath local contact.
- In this work, the modification of rear side parameters of Bi-PERCs was found to modify the Al-BSF thickness, and final quality of surface passivation level and Si bulk. All these critical measurement parameters significantly impacted the V_{oc} and FF of a cell and play important roles in regulating high-yield of Bi-PERC performance.

Conclusion

We utilized the micro-PL imaging technique to map the evidence of metallization-induced recombination losses relating with the Al-Si interdiffusion behavior during contact firing of Bi-PERCs.

- The results from micro-PL images show that the differences in Al rear grid width relating to the fractions of metallization area had significantly modified the Al-Si interdiffusion behavior thereby affecting the Al-BSF thickness, final quality of surface passivation level and Si bulk.
- Particularly, the latter one (quality of Si substrate) was first observed in this study and it can be detected by micro-PL imaging technique.

References

[1] S. Joonwichien M. Moriya, S. Utsunomiya, Y. Kida, K. Shirasawa, and H. Takato, IEEE J. Photovolt., vol. 10 (2), pp. 407–416, 2020.
[2] S. Joonwichien, K. Shirasawa, and H. Takato, “Al-Si interdiffusion role in determining metallization-induced recombination losses of bifacial solar cell,” To be submitted
[3] S. Joonwichien, S. Utsunomiya, M. Moriya, Y. Kida, K. Shirasawa, and H. Takato, in Proc. 47th Int. IEEE PVSC (2020).
[4] M. Tajima, Y. Iwata, F. Okayama, H. Toyota, H. Onodera, and T. Sekiguchi, J. Appl. Phys. 111, pp. 113523, 2012.
[5] T. Trupke, R.A. Bardos, M.C. Schubert, and W. Warta, Appl. Phys. Lett. 89, pp. 044107-1–044107-3, 2006.
[6] H. Sugimoto, M. Inoue, M. Tajima, A. Ogura, and Y. Ohshita, Jpn. J. Appl. Phys. 45, pp. L641–L643, 2006.
[7] R.A. Street, Adv. Phys. 30, pp. 593–676, 1981.
[8] T. Searle, in Properties of Amorphous Si and its Alloys, edited by T. Searle, p. 235, NSPEC, United Kingdom, 1998.
[9] I. Guler, Mat. Sci. Eng. B-Adv. 246, pp. 21–26, 2019.
[10] B. Hallam, B. Tjahjono, T. Trupke, and S. Wenham, J. Appl. Phys. 115, 044901, 2014.
[11] S. Joonwichien M. Moriya, S. Utsunomiya, Y. Kida, K. Shirasawa, and H. Takato, IEEE J. Photovolt., vol. 8 (1), pp. 54–58, 2018.